

Chiral condensate and Dirac spectrum of one- and two-flavor QCD at nonzero θ -angle

Mario Kieburg¹, Jacobus Verbaarschot^{2,*}, and Tilo Wettig³

¹*Department of Physics, University of Bielefeld, 33501 Bielefeld, Germany*

²*Department of Physics and Astronomy, Stony Brook University, New York 11794, USA*

³*Department of Physics, University of Regensburg, 93040 Regensburg, Germany*

Abstract. In previous work we showed that the chiral condensate of one-flavor QCD exhibits a Silver Blaze phenomenon when the quark mass crosses $m = 0$: the chiral condensate remains constant while the quark mass crosses the spectrum of the Dirac operator, which is dense on the imaginary axis. This behavior can be explained in terms of exponentially large cancellations between contributions from the zero modes and from the nonzero modes when the quark mass is negative. In these proceedings we show that a similar Silver Blaze phenomenon takes places for QCD with one flavor and arbitrary θ -angle, and for QCD with two flavors with different quark masses m_1 and m_2 . In the latter case the chiral condensate remains constant when m_1 crosses zero at fixed $m_2 > 0$ until the Dashen point $m_1 = -m_2$ is reached, where the chiral condensate has a discontinuity. In terms of contributions from the Dirac spectrum the shift of the discontinuity from $m_1 = 0$ to $m_1 = -m_2$ also arises from exponentially large cancellations between the zero and nonzero modes when $m_1 m_2 < 0$. All calculations are performed in the microscopic or ε -domain of QCD. Results for arbitrary θ -angle are discussed as well.

1 Introduction

Although the experimental value of the θ -angle is consistent with zero, the θ -dependence of the QCD partition function has attracted a great deal of attention since the early days of QCD [1, 2] and also in lattice QCD [3, 4]. One reason is the close connection with topology. For example, the topological susceptibility can be obtained from the second derivative of the partition function with respect to θ . The θ -dependence of the QCD partition function also makes it possible to isolate the partition function at fixed topological charge [5], which was the starting point for the connection between chiral random matrix theory and QCD [6].

Another reason for considering a nonzero θ -angle is to study the effect of negative quark masses, which is equivalent to $\theta = \pi$. For one flavor the chiral condensate is constant when the quark mass changes sign (see Fig. 1). This raises the question of what happens to the spectrum of the Dirac operator at $\theta = \pi$ or when the quark mass crosses the imaginary axis [7] and how one can reconcile this property with the Banks-Casher relation [8]. For two flavors, the Dashen phenomenon [9–13] has a long history. It occurs when the sum of the quark masses vanishes, or for equal quark masses

*Speaker, e-mail: jacobus.verbaarschot@stonybrook.edu

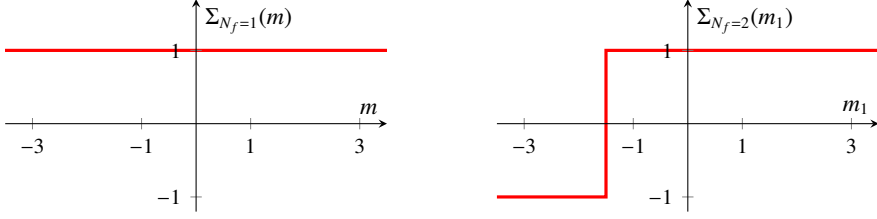


Figure 1. Behavior of the chiral condensate (in suitable units) for $N_f = 1$ (left) and $N_f = 2$ (right, with $m_2 = 1.5$).

at $\theta = \pi$. At this point, the chiral condensate changes sign, and one of the questions we have been interested in is to explain the phase diagram shown in the plane of the two quark masses (see Fig. 2) in terms of the spectrum of the Dirac operator.

In the ε -domain of QCD the exact analytical form of the spectral density of the Dirac operator as well as the partition function at fixed topological charge ν are given by expressions in terms of Bessel functions that can be derived from chiral random matrix theory [14–16]. It is possible to evaluate the sums over ν [17, 18], which provides us with exact analytical results for the spectral density at fixed θ -angle and allows us to study the connection between the spectral density and the chiral condensate at fixed θ -angle. In [17, 19] this program was carried out for $N_f = 1$ and θ equal to 0 or π . In these proceedings we will investigate the same questions for both $N_f = 1$ and $N_f = 2$ at arbitrary θ -angle. More details will be discussed in a forthcoming paper [18].

2 Chiral condensate for one- and two-flavor QCD

The θ -dependence of the one-flavor QCD partition function is given by

$$Z(m, \theta) = \sum_{\nu} e^{i\nu\theta} Z_{\nu}(m) \quad \text{with} \quad Z_{\nu}(m) = \left\langle \prod_k (i\lambda_k + m) \right\rangle_{\nu} = m^{|\nu|} \left\langle \prod_{\lambda_k > 0} (\lambda_k^2 + m^2) \right\rangle_{\nu}, \quad (1)$$

where the average is over gauge field configurations with topological charge ν , m is the quark mass (which we assume to be real), and the $i\lambda_k$ are the eigenvalues of the anti-Hermitian Dirac operator (which are either zero or occur in pairs $\pm i\lambda_k$). Note that a negative quark mass can be interpreted as $\theta \rightarrow \theta + \pi$ and visa versa. The partition function for fixed topological charge follows by Fourier inversion,

$$Z_{\nu}(m) = \frac{1}{2\pi} \int_{-\pi}^{\pi} d\theta e^{-i\nu\theta} Z(m, \theta). \quad (2)$$

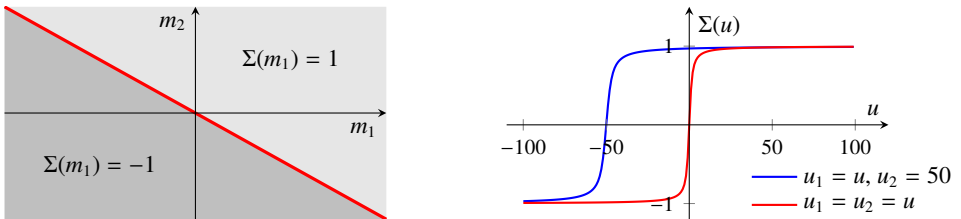


Figure 2. Left: phase diagram of the chiral condensate for QCD with two flavors in the plane of the two quark masses at $\theta = 0$. Right: mass dependence of the chiral condensate at $\theta = 0$ when both masses are equal (red curve) and when one of the masses is kept fixed (blue curve). We used the notation $u = mV\Sigma$.

For one-flavor QCD, chiral symmetry is broken by the anomaly, there is no spontaneous symmetry breaking, and there are no Goldstone bosons. The mass dependence of the one-flavor QCD partition function is given by [5]

$$Z(m, \theta) = e^{mV\Sigma \cos \theta + O(m^2 V)}, \quad (3)$$

where V is the volume and Σ is the absolute value of the chiral condensate in the limit $m = 0$ and $\theta = 0$. The chiral condensate is defined as

$$\Sigma(m) = -\langle \bar{q}q \rangle = \frac{1}{V} \frac{d}{dm} \log Z(m) = \left\langle \frac{1}{V} \sum_k \frac{1}{i\lambda_k + m} \right\rangle, \quad (4)$$

where the average includes the fermion determinant. This definition is valid for both fixed v and fixed θ . Equations (3) and (4) imply that the condensate as a function of θ vanishes for $\theta = \pi/2$, which will be discussed in detail in the next section.

The two-flavor partition function is

$$Z(m_1, m_2, \theta) = \sum_v e^{iv\theta} (m_1 m_2)^{|v|} \left\langle \prod_{\lambda_k \neq 0} (i\lambda_k + m_1)(i\lambda_k + m_2) \right\rangle_v, \quad (5)$$

where we again assume that the masses are real. The behavior of the chiral condensate shown in Fig. 2 can be understood simply in terms of the chiral Lagrangian. The mean-field result for the two-flavor partition function at $\theta = 0$ is given by

$$Z(m_1, m_2, \theta = 0) = \int_{U \in \text{SU}(2)} dU e^{V\Sigma \text{tr}[\text{diag}(m_1, m_2)(U + U^{-1})]}. \quad (6)$$

In the thermodynamic limit U aligns itself with the mass term, resulting in [5]

$$Z(m_1, m_2, \theta = 0) = e^{V\Sigma|m_1 + m_2|}. \quad (7)$$

The chiral condensate is then

$$\Sigma(m_1, \theta = 0) = -\langle \bar{q}_1 q_1 \rangle = \frac{1}{V} \frac{d}{dm_1} \log Z(m_1, m_2, \theta = 0) = \Sigma \text{sign}(m_1 + m_2), \quad (8)$$

which is the behavior shown in Figs. 1 (right) and 2.

Both for one-flavor QCD and for two-flavor QCD with different masses, the chiral condensate does not have a discontinuity when the quark mass crosses the line of eigenvalues, which also for nonzero θ are dense on the imaginary axis. This remarkable property seems to violate the Banks-Casher relation, which is derived starting from the RHS of (4). Due to the symmetries of the λ_k , the sum changes sign when $m \rightarrow -m$. Apparently, this sign change gets compensated by the sign of the fermion determinant in the measure, which can be negative when $m < 0$ or $m_1 m_2 < 0$. A similar ‘‘Silver Blaze phenomenon’’ arises for QCD at nonzero chemical potential, where the chiral condensate remains constant while the Dirac spectrum is strongly altered by the chemical potential [20–22]. The motivation to study QCD at nonzero θ -angle came from the desire to understand this Silver Blaze behavior of the chiral condensate in terms of the Dirac spectrum, but also to clarify statements in the literature on the spectral density of the Dirac operator [7]. Since QCD at nonzero θ -angle also has a severe sign problem, see Fig. 3 (left), we expect that the explanation of this behavior will be similar to that of QCD at nonzero chemical potential, where it was found that the apparent discontinuity of the chiral condensate can be moved by a strongly oscillating and exponentially increasing spectral density [21].

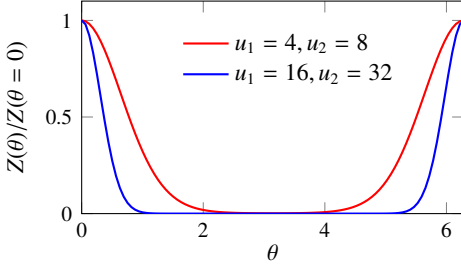


Figure 3. Severity of the sign problem for two flavors as given by $Z(m_1, m_2, \theta)/Z(m_1, m_2, \theta = 0)$, to leading order in chiral perturbation theory.

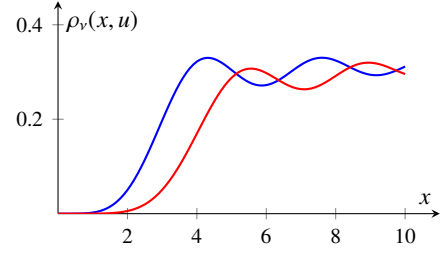


Figure 4. One-flavor microscopic spectral density for $v = 2$ and $u = mV\Sigma = 1$ (red) compared to the quenched result for $v = 2$ (blue).

3 Dirac spectrum and chiral condensate for $N_f = 1$

The spectral density of the Dirac operator at fixed θ -angle is given by

$$\rho(\lambda, m, \theta) = \sum_v P_v \rho_v(\lambda, m), \quad P_v = \frac{e^{iv\theta} Z_v(m)}{Z(m, \theta)}, \quad (9)$$

where P_v is the statistical weight to find a gauge field configuration with topological charge v . Note that for $\theta \neq 0$ and/or $m < 0$ the partition function is not positive definite and $\rho(\lambda, m, \theta)$ may become negative. The chiral condensate is still given by

$$\Sigma(m) = \frac{1}{V} \int_{-\infty}^{\infty} d\lambda \frac{\rho(\lambda)}{i\lambda + m}. \quad (10)$$

The spectral density $\rho(\lambda)$ will be decomposed into a zero-mode part and a nonzero-mode part, the latter being the sum of a “quenched” and a “dynamical” part,

$$\begin{aligned} \rho(\lambda) &= \rho_{\text{zm}}(\lambda) + \rho_{\text{nz}}(\lambda) \\ &= \delta(\lambda) \sum_v |\nu| P_v + \rho_q(\lambda) + \rho_d(\lambda). \end{aligned} \quad (11)$$

The quenched part at fixed θ is obtained via (9) from the quenched part at fixed v . While the latter does not depend on the mass, $\rho_q(\lambda)$ at fixed θ does since P_v does, see (14) below.

We will do our calculations in the microscopic domain of QCD, where analytical results for the spectral density are given by chiral random matrix theory. In this domain, also known as the ε -domain, the quark mass and the Dirac eigenvalues scale as $m \sim 1/V$ and $\lambda \sim 1/V$ in the thermodynamic limit. Correction terms will enter when m, λ are no longer small compared to $1/\Lambda_{\text{QCD}} \sqrt{V}$. The one-flavor spectral density in the ε -domain is given by [23, 24]

$$\rho_v(x, u) = |\nu| \delta(x) + \frac{|x|}{2} [J_v^2(x) - J_{v+1}(x) J_{v-1}(x)] - \frac{|x|}{x^2 + u^2} \left[x J_v(x) J_{v+1}(x) + u \frac{I_{v+1}(u)}{I_v(u)} J_v^2(x) \right], \quad (12)$$

where $x \equiv \lambda \Sigma V$ and $u \equiv m \Sigma V$. An example is shown in Fig. 4. The spectral density at fixed θ -angle is

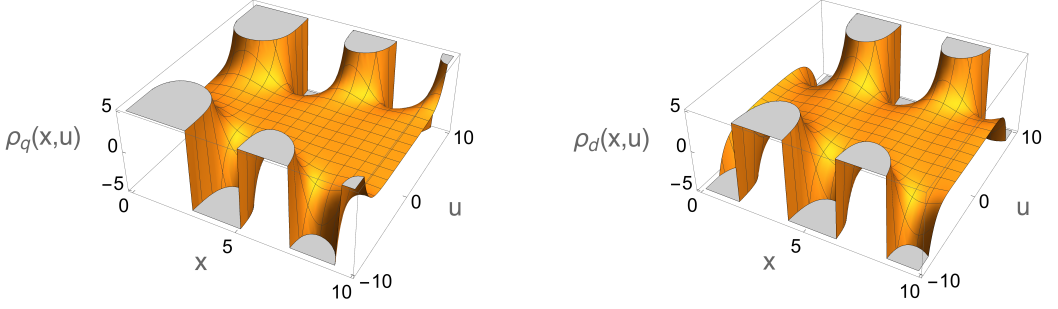


Figure 5. Spectral density of the Dirac operator for one-flavor QCD at $\theta = \pi/2$. Left: quenched part, right: dynamical part.

obtained by summing over ν , resulting in [18]

$$\rho_{zm}(x, u, \theta) = -\delta(x) \int_{-\pi}^{\pi} \frac{d\varphi}{4\pi \sin^2 \frac{\varphi}{2}} \frac{e^{u \cos(\theta+\varphi)} - e^{u \cos \theta}}{e^{u \cos \theta}}, \quad (13)$$

$$\rho_q(x, u, \theta) = \int_{-\pi}^{\pi} \frac{d\varphi}{4\pi \sin^2 \frac{\varphi}{2}} \frac{e^{u \cos(\theta+\varphi)}}{e^{u \cos \theta}} J_1(2|x| \sin \frac{\varphi}{2}), \quad (14)$$

$$\rho_d(x, u, \theta) = \frac{|x|}{x^2 + u^2} \int_{-\pi}^{\pi} \frac{d\varphi}{2\pi} \frac{e^{u \cos(\theta+\varphi)}}{e^{u \cos \theta}} \left[i x e^{i\varphi/2} J_1(2x \sin \frac{\varphi}{2}) - u e^{-i(\theta+\varphi)} J_0(2x \sin \frac{\varphi}{2}) \right], \quad (15)$$

where (13) is a principal-value integral. In Fig. 5 we show ρ_q and ρ_d for $\theta = \pi/2$ as a function of u and x . For increasing absolute value of u , we observe oscillations with an amplitude that grows exponentially with the volume and a period on the order of the inverse volume. The chiral condensate corresponding to this spectral density should vanish (since $\theta = \pi/2$)! In Fig. 6 we see that both the quenched and the zero-mode contributions to the chiral condensate increase exponentially with the volume, while the dynamical part remains finite. The leading-order contributions of an asymptotic expansion in $1/V$ cancel [22],

$$\Sigma_q \sim \frac{\text{sign}(m) e^{|m|V\Sigma}}{\sqrt{2\pi}|m|^{3/2}} [1 + O(1/mV\Sigma)], \quad \Sigma_{zm} \sim -\frac{\text{sign}(m) e^{|m|V\Sigma}}{\sqrt{2\pi}|m|^{3/2}} [1 + O(1/mV\Sigma)]. \quad (16)$$

In fact this cancellation holds to all orders in $1/mV\Sigma$, and the sum of the quenched part and the zero-mode part is finite [18].

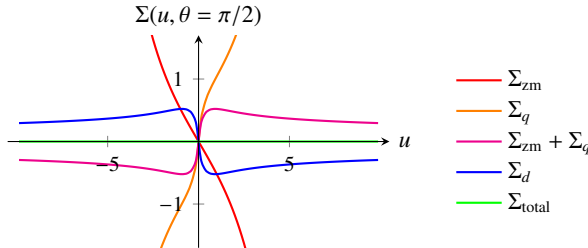


Figure 6. Contributions to the chiral condensate for one-flavor QCD at $\theta = \pi/2$.

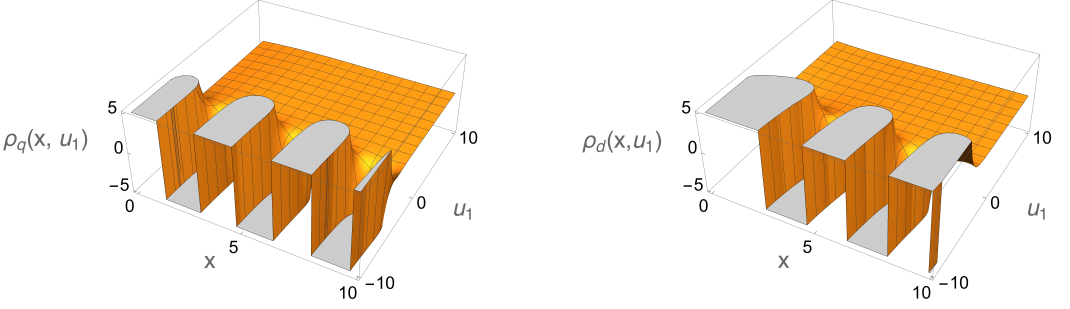


Figure 7. Spectral density of the QCD Dirac operator for two flavors and $\theta = 0$ with $u_2 = 10$. Left: quenched contribution, right: correction induced by the fermion determinant.

4 Dirac spectrum and chiral condensate for $N_f = 2$

For $N_f = 2$ it is also possible to perform the sum over ν to obtain the spectral density of the Dirac operator at fixed θ -angle. The nonzero-mode part reads

$$\begin{aligned} \rho_{\text{nz}}(x, u_1, u_2, \theta) = & \frac{|x|}{Z(u_1, u_2, \theta)} \int_{-\pi}^{\pi} \frac{d\varphi}{2\pi} \left\{ \frac{J_1(2x \sin \frac{\varphi}{2})}{2x \sin \frac{\varphi}{2}} Z(u_1, u_2, \theta - \varphi) \right. \\ & + \frac{ixe^{i(\varphi/2 - \theta)}(2u_1u_2 - (u_1^2 + u_2^2)e^{i(\theta - \varphi)})}{(x^2 + u_1^2)(x^2 + u_2^2)} J_1(2x \sin \frac{\varphi}{2}) Z(u_1, u_2, \theta - \varphi) \\ & \left. - \frac{J_0(2x \sin \frac{\varphi}{2})}{(x^2 + u_1^2)(x^2 + u_2^2)} I_0 \left(\sqrt{u_1^2 + u_2^2 + 2u_1u_2 \cos(\theta - \varphi)} \right) (u_1u_2 e^{-i(\theta - \varphi)} + x^2 e^{-i\varphi}) \right\}, \end{aligned} \quad (17)$$

where the first line corresponds to the quenched part and the rest to the dynamical part. In Fig. 7 we show these two parts separately as a function of x and u_1 for $u_2 = 10$ and $\theta = 0$. Again we observe exponentially large oscillations for $u_1 < 0$, this time only for negative quark mass because $\theta = 0$. The zero-mode contribution to the spectral density is given by the principal-value integral

$$\rho_{\text{zm}}(x, u_1, u_2, \theta) = -\delta(x) \int_{-\pi}^{\pi} \frac{d\varphi}{4\pi \sin^2 \frac{\varphi}{2}} \frac{Z(u_1, u_2, \theta - \varphi) - Z(u_1, u_2, \theta)}{Z(u_1, u_2, \theta)}. \quad (18)$$

For large volume the integrand of (18) is dominated by $\varphi = \tilde{\theta}$, with $\tilde{\theta} = \theta$ for $u_1u_2 > 0$ and $\tilde{\theta} = \theta + \pi$ for $u_1u_2 < 0$, resulting in the asymptotic contribution to the chiral condensate of the first quark

$$\Sigma_{\text{zm}}(u_1, u_2, \theta) \sim -\frac{1}{4\pi u_1 \sin^2 \frac{\tilde{\theta}}{2}} \frac{Z(u_1, u_2, \theta - \tilde{\theta})}{Z(u_1, u_2, \theta)} \quad (\text{valid for } \tilde{\theta} \text{ away from } 0 \bmod 2\pi), \quad (19)$$

which grows exponentially with the volume since for $\tilde{\theta} \neq 0$ the free energy of the denominator is less than the free energy of the numerator. Since the sum of the zero-mode part and the quenched part of the chiral condensate is finite for $V \rightarrow \infty$, the quenched part should also grow exponentially but with the opposite sign. It is given by

$$\Sigma_q(u_1, u_2, \theta) = \int_{-\pi}^{\pi} d\varphi \frac{1 - 2|u_1 \sin \frac{\varphi}{2}| K_1(2|u_1 \sin \frac{\varphi}{2}|)}{4\pi u_1 \sin^2 \frac{\varphi}{2}} \frac{Z_2(u_1, u_2, \theta - \varphi)}{Z_2(u_1, u_2, \theta)}. \quad (20)$$

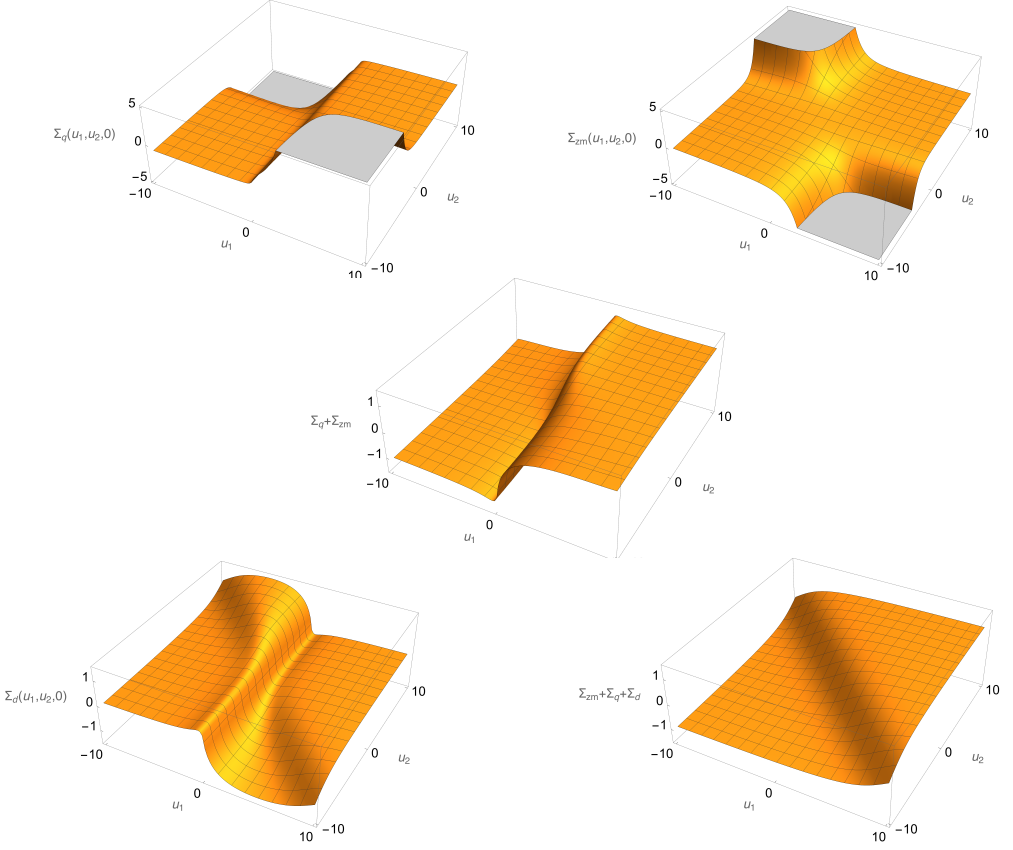


Figure 8. Contributions to the chiral condensate for two-flavor QCD at $\theta = 0$. The contributions of the quenched part and the zero-mode part of the spectral density increase exponentially with the volume when the product of the quark masses is negative (upper figures). However, their sum remains finite (central figure), and after adding the dynamical part we observe a discontinuity on the line $u_1 + u_2 = 0$.

For large V this simplifies to

$$\Sigma_q(u_1, u_2, \theta) \sim \frac{1}{4\pi u_1 \sin^2 \frac{\tilde{\theta}}{2}} \frac{Z_2(u_1, u_2, \theta - \tilde{\theta})}{Z_2(u_1, u_2, \theta)} \quad (\text{valid for } \tilde{\theta} \text{ away from } 0 \bmod 2\pi), \quad (21)$$

which exactly cancels the exponentially increasing contribution from the zero modes. One can show that this cancellation works to all orders [18]. In Fig. 8 we show that both the quenched and the zero-mode contributions to the chiral condensate grow exponentially for $u_1 u_2 < 0$ (upper two figures), but that their sum is finite (central figure). The discontinuity shown in Fig. 2 is recovered after adding the dynamical contribution (lower figures).

5 Conclusions

In the ε -domain of QCD we have obtained exact analytical expressions for the eigenvalue density of the Dirac operator at fixed $\theta \neq 0$ for both one and two flavors. These results made it possible to

explain how the different contributions to the spectral density conspire to give a chiral condensate at fixed θ that does not change sign when the quark mass (or one of the quark masses for two flavors) crosses the imaginary axis, while the chiral condensate at fixed topological charge does change sign. From QCD at nonzero density we have learnt that the discontinuity of the chiral condensate may move to a different location when the spectral density increases exponentially with the volume with oscillations on the order of the inverse volume. This is indeed what happens when the product of the quark masses becomes negative, but the situation is more subtle in this case: the contribution of the “quenched” part of the spectral density diverges in the thermodynamic limit at nonzero θ , but this divergence is canceled exactly by the contribution from the zero modes. We conclude that the zero modes are essential for the continuity of the chiral condensate and that their contribution has to be perfectly balanced against the contribution from the nonzero modes. Lattice simulations at nonzero θ -angle can only be trusted if this is indeed the case.

This work was supported in part by DFG grant AK35/2-1 (MK), U.S. DOE grant No. DE-FAG-88FR40388 and the Alexander von Humboldt Foundation (JV), and DFG grant SFB/TRR-55 (TW).

References

- [1] G. 't Hooft, *Extended Objects in Gauge Field Theories*, in *t'Hooft, G. (ed.): Under the spell of the gauge principle 254-287*, and *Banff 1977, Proceedings, Summer Institute on Particles and Fields 165-198* (1977)
- [2] D. Gaiotto, A. Kapustin, Z. Komargodski, N. Seiberg, *JHEP* **05**, 091 (2017), 1703.00501
- [3] V. Azcoiti, G. Di Carlo, A. Galante, V. Laliena, *Phys. Rev. Lett.* **89**, 141601 (2002), hep-lat/0203017
- [4] V. Azcoiti, G. Di Carlo, E. Follana, E. Royo-Amondarain, A.V. Avilés-Casco (2017), 1709.07667
- [5] H. Leutwyler, A.V. Smilga, *Phys. Rev.* **D46**, 5607 (1992)
- [6] E.V. Shuryak, J.J.M. Verbaarschot, *Nucl. Phys.* **A560**, 306 (1993), hep-th/9212088
- [7] M. Creutz, *Annals Phys.* **322**, 1518 (2007), hep-th/0609187
- [8] T. Banks, A. Casher, *Nucl. Phys.* **B169**, 103 (1980)
- [9] R.F. Dashen, *Phys. Rev.* **D3**, 1879 (1971)
- [10] G. Akemann, J.T. Lenaghan, K. Splittorff, *Phys. Rev.* **D65**, 085015 (2002), hep-th/0110157
- [11] J. Lenaghan, T. Wilke, *Nucl. Phys.* **B624**, 253 (2002), hep-th/0108166
- [12] S. Aoki, M. Creutz, *Phys. Rev. Lett.* **112**, 141603 (2014), 1402.1837
- [13] D.P. Horkel, S.R. Sharpe, *Phys. Rev.* **D92**, 094514 (2015), 1507.03653
- [14] J.J.M. Verbaarschot, *Phys. Rev. Lett.* **72**, 2531 (1994), hep-th/9401059
- [15] J.J.M. Verbaarschot, T. Wettig, *Ann. Rev. Nucl. Part. Sci.* **50**, 343 (2000), hep-ph/0003017
- [16] J.J.M. Verbaarschot, in *The Oxford Handbook of Random Matrix Theory*, edited by G. Akemann, J. Baik, P. Di Francesco (Oxford University Press, 2010), 0910.4134
- [17] J.J.M. Verbaarschot, T. Wettig, *Phys. Rev.* **D90**, 116004 (2014), 1407.8393
- [18] M. Kieburg, J. Verbaarschot, T. Wettig, *Dirac spectrum and chiral condensate of QCD at fixed θ -angle* (in preparation)
- [19] J. Verbaarschot, T. Wettig, *PoS LATTICE2014*, 072 (2014), 1412.5483
- [20] T.D. Cohen, *Phys. Rev. Lett.* **91**, 222001 (2003), hep-ph/0307089
- [21] J.C. Osborn, K. Splittorff, J.J.M. Verbaarschot, *Phys. Rev. Lett.* **94**, 202001 (2005), hep-th/0501210
- [22] T. Kanazawa, T. Wettig, N. Yamamoto, *JHEP* **12**, 007 (2011), 1110.5858

- [23] P.H. Damgaard, S.M. Nishigaki, Nucl.Phys. **B518**, 495 (1998), hep-th/9711023
- [24] T. Wilke, T. Guhr, T. Wettig, Phys.Rev. **D57**, 6486 (1998), hep-th/9711057